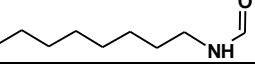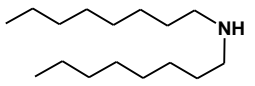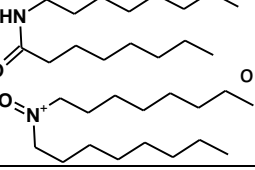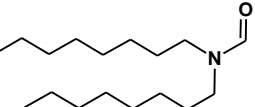# An Experimental and Computational Look at the Radiolytic Degradation of TODGA and the Effect on Metal Complexation

Ashleigh Kimberlin[a], Dominique Guillaumont[a], Sylvie Arpigny[a], Béatrice Camès[a], Philippe Guilbaud[a], Georges Saint-Louis[a], Hitos Galán[b], and Laurence Berthon*[a]

Supplemental

Table S1: Complete list of peaks found in ESI-MS spectra. Some peaks remain unassigned. The numbers refer to the solution conditions detailed in Table 1. The conditions are also listed under the name where octOH = 5 %$_{Vol}$ 1-octanol, x mol L^{-1} HNO$_3$ = concentration of HNO$_3$ in the precontact, even numbers being irradiated to approx. 250 kGy and odd numbers being irradiated to approx. 500 kGy. Nd refers to if the product has appeared in an ion peak with Nd^{3+}. References are literature sources in which the degradation product has previously been identified as a radiolysis product of DGA. Main degradation products and degradation products found in Nd molecular ion peaks have been given a DP number.

DP	Proposed Structure	LH$^+$ m/z	LNa$^+$ m/z	0	1/2	3/4 OctOH	5/6 1 mol L^{-1} HNO$_3$	7/8 octOH 1 mol L^{-1}	9/10 OctOH 2.5 mol L^{-1}	Nd	Comments	Ref.
I		130	152		*	*	*	*	*		High instrument response factor	
II		157	179		*	*	*	*	*			
		194					*	*	*			
		200							*			
		210					*	*	*			
		240			*	*			*			
III		242	264	*	*	*	*	*	*		High instrument response factor	1-7
		255					*		*			
IV	or	256	278				*	*	*		Oxygen location debatable Only visible at 250 kGy	2
		267	289		*	*	*	*	*			
V		270	292		*	*	*	*	*			1-8

| Label	Structure	m/z	m/z	1	2	3	4	5	6	7	X	Notes	Ref
VI	dioctyl-N-acetyl amide	284	306		*	*	*		*	*			1-8
VII	dioctyl-N-(hydroxyacetyl) amide (OH)	300	322		*	*	*		*	*		May complex metal in solution, see discussion	1-8
	methoxyacetyl amide with double bond	312	334	*	*	*	*		*	*		location of double bond unknown	
VIII	methoxyacetyl amide	314	336	*	*	*	*		*	*		Results from radiolytic split	1, 8
		320						*	*	*			
		338						*	*	*			
		340			*								
IX	dioctyl amide, –O–CH$_2$COOH	358	380					*	*		X	Mostly seen as Na$^+$ adduct, see Figure 4 for formation mechanism	1, 3, 5-8
		368			*	*				*			
		379						*	*	*			
		468	490		*	*							
X	amide, –O–CH$_2$CO–NH–octyl	469	491	*	*	*	*		*	*	X	LK$^+$: 507	3-6, 8
XI	amide, –O–CH$_2$CO–OC_8H_{17}	470	492	*			*			*	X	LK$^+$: 508 See Figure 4 for formation mechanism	3
		550	572		*	*	*		*	*			
		555			*	*	*						
	diamide (diglycolamide)	567	589	*	*	*	*		*	*			
	TODGA	581	603	*	*	*	*		*	*		LK$^+$: 619	
XII	diamide with carbonyl	595	617		*	*	*		*	*	X	LK$^+$: 633	
		654						*	*	*			
		710			*	*	*		*	*			
XIII	diamide, $H_{25}C_{12}$	751	773								X	Only seen in Nd complexes, dodecyl location variable	
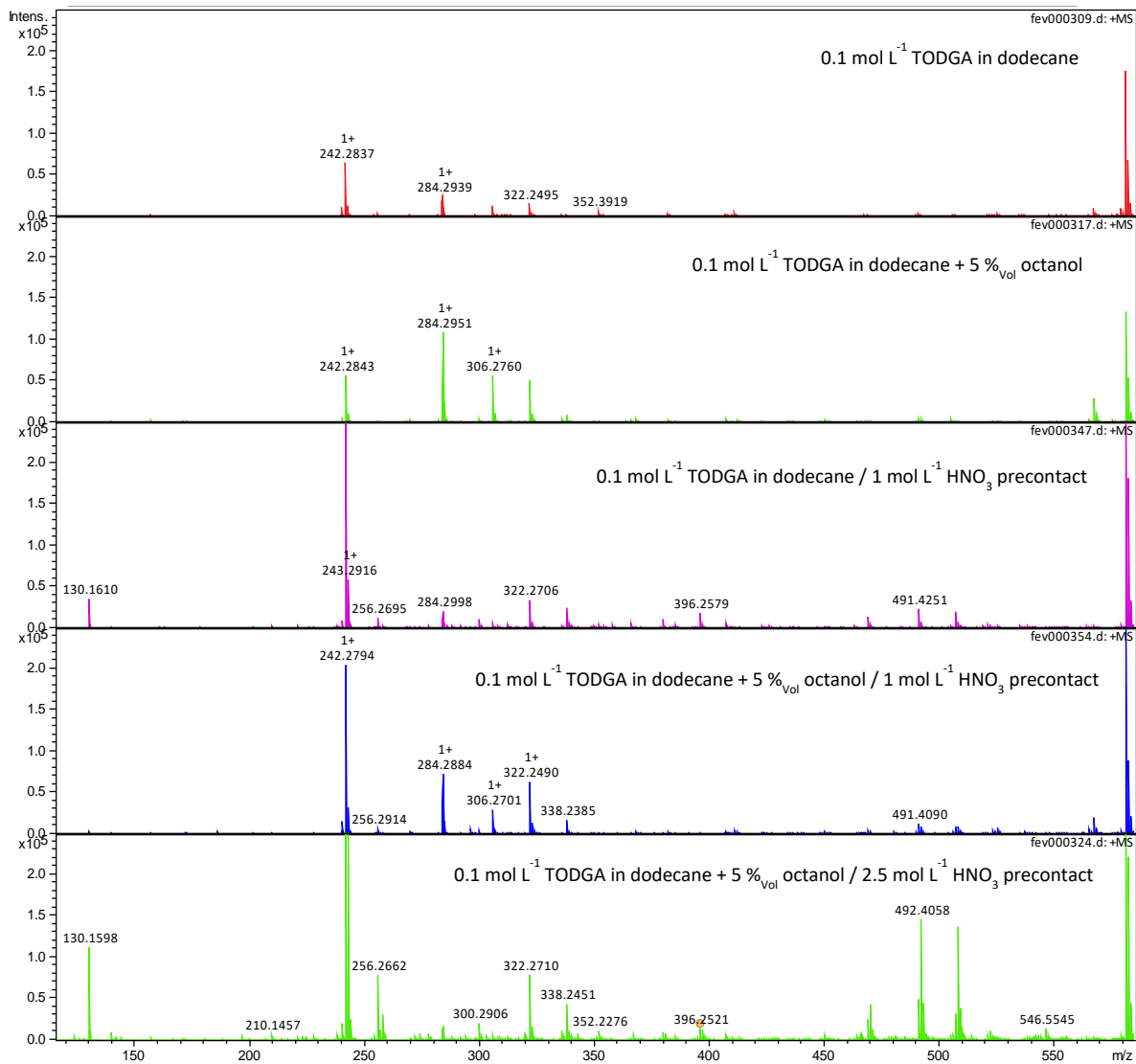
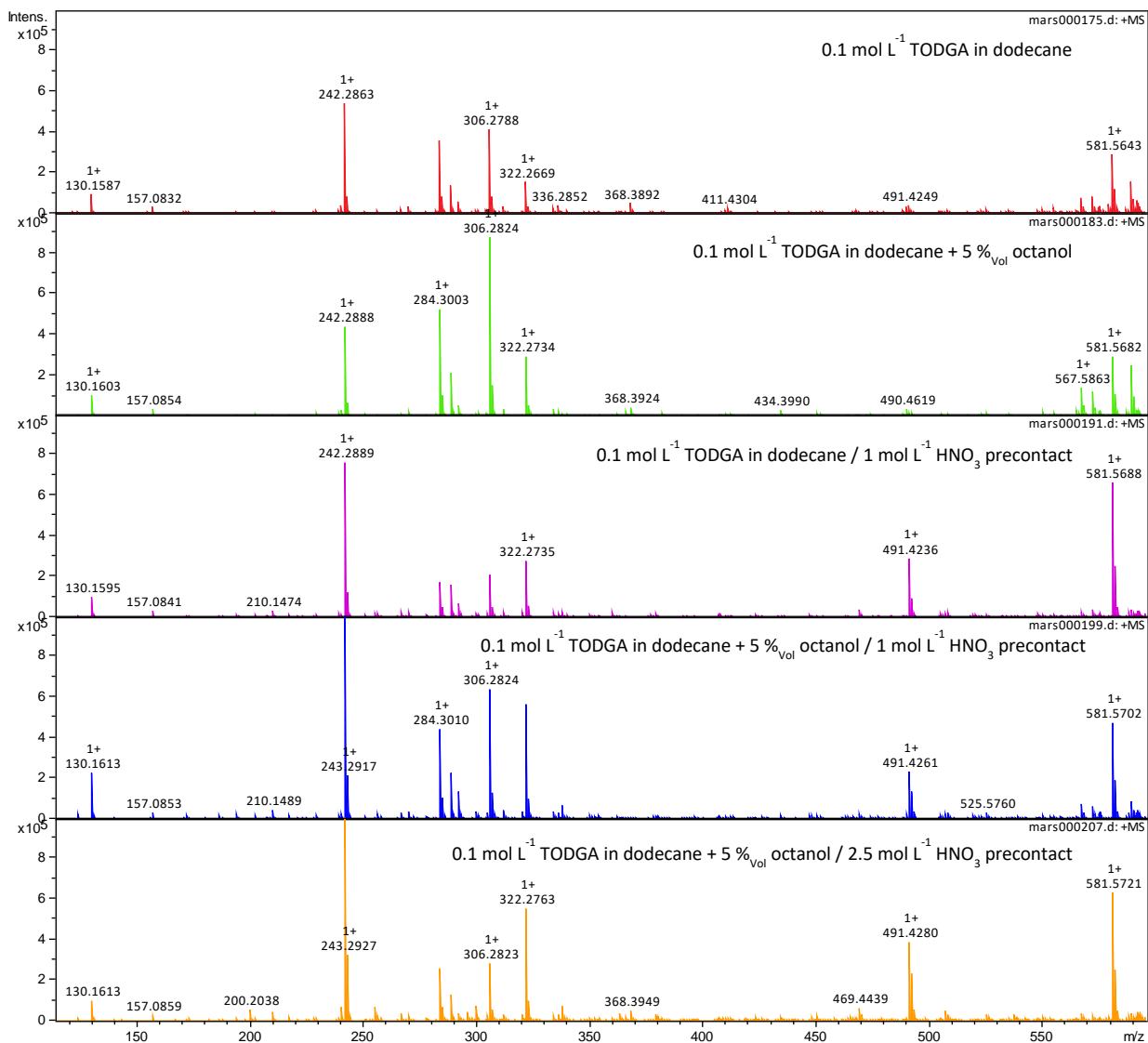Figure S1: ESI-MS of TODGA solutions irradiated to 250 kGy after dilution in 1/10000th in acetonitrile.

Figure S2: ESI-MS of TODGA solution irradiated to 500 kGy after dilution in 1/10000th in acetonitrile

Bond	Dissociation Energy (eV)
N_{amide}-C_1	3.81
C_1-C_2	3.61
C_2C_3	3.89
C_3-C_4	3.82
C_4-C_5	3.82
C-$_5$-C_6	3.86
N_{amide}-C_9	3.96
C_9-C_{10}	3.34
C_{10}-O_{ether}	3.31
C_{10}-H_9	3.64
C_5-H_5	4.29
C_4-H_4	4.25
C_3-H_3	4.28
C_2-H_2	4.30
C_1-H_1	4.00

Figure S3: Schematic representation of molecule used in TODGA and bond dissociation energy calculations.

Bond dissociation energies of TODGA were calculated using Gaussian 16. The energies of the two fragments formed by the hemolytic cleavage of bond were calculated using the G3MP2 method. The difference in total energy of the fragments and the whole molecule is the bond dissociation energy. To reduce computation time, the bond dissociation energies for TEDGA were calculated for the center of the molecule, three of the octyl chains in TODGA were replaced with ethyl chains when calculating the alkyl C-C bond dissociation energies, and the alpha-hydroxyamide half of TODGA was used for the calculation of C-H bonds in the alkyl chains.

The weakest bond in the molecule is between the etheric C and O. The amide C-N bond is the strongest, therefore least likely to be broken by direct excitation, i.e. being attacked by a dodecane radical. The alkyl chains, for the most part, have the same high energy, making fragmentation of the alkyl chain more unlikely than fragmentation closer to the polar center of the molecule. The bond between the first (C_1) and second (C_2) carbons on the alkyl chain seems unusually weak, considering that the adjacent amide would strengthen the C_1-N bond, but not weaken the next bond. This result is due to the computational method used, as each fragment made by the hemolytic cleavage of the bond is calculated separately. The fragment containing the amide is stabilized due to the presence of a partial double bond ($\bullet CH_2 \approx N$-$C=O$), which causes the overall energy of that fragment to decrease.
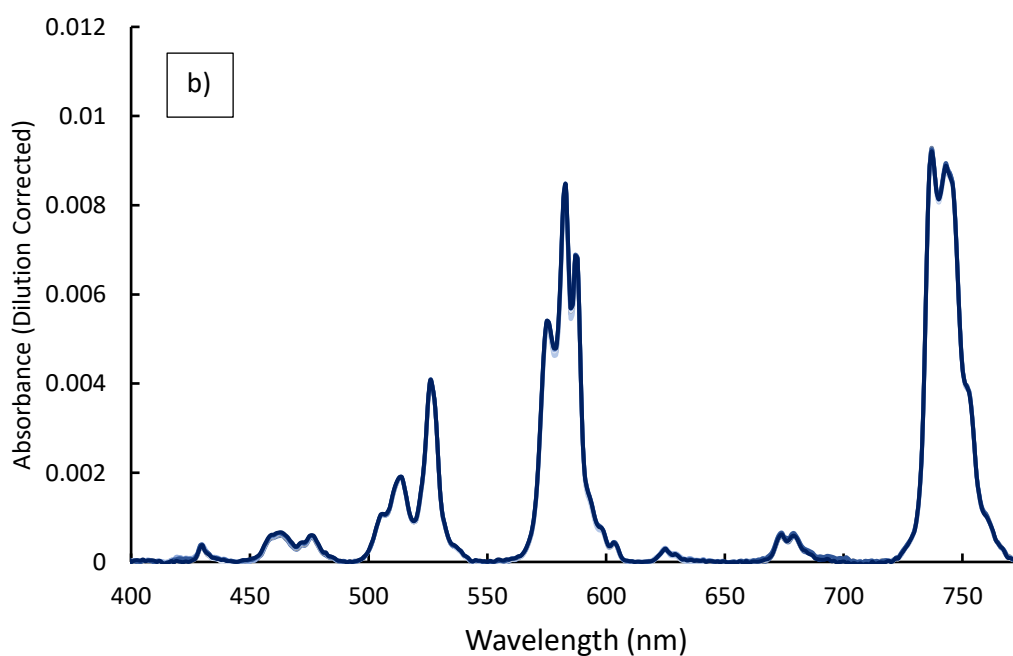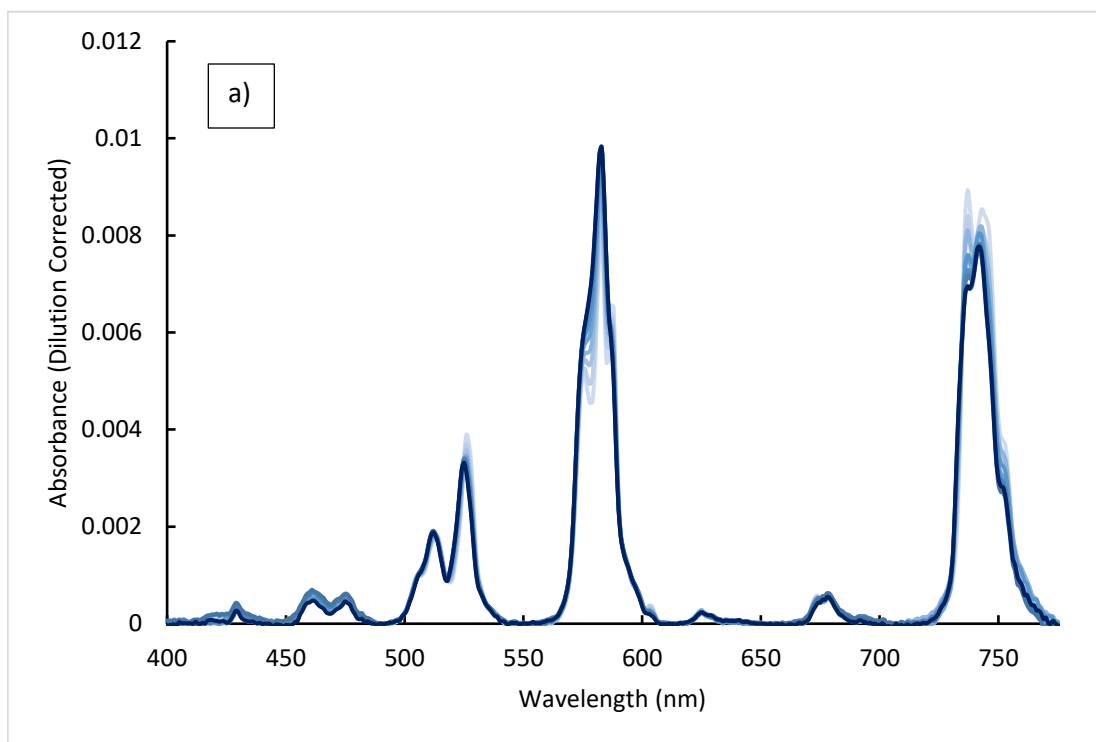
Figure S4: UV-Vis spectra of Nd-TODGA solutions in n-dodecane + 5 %$_{Vol}$ 1-octanol with either DPVII (a) or DPIX (b). In the top, the color progresses from light to dark as DPVII is added. Initial solution: 0.1 mol L^{-1} TODGA in dodecane + 5 %$_{Vol}$ 1-octanol solution containing 18 mmol L^{-1} Nd. Progressive addition of 0.1 mL of 0.1 mol L^{-1} DPVII (top) or DPIX (bottom) in 0.1 mol L^{-1} TODGA solution until a 1:1 mol ratio of TODGA to the degradation product was reached. Final concentration 0.05 mol L^{-1} TODGA + 0.05 mol L^{-1} DPVII (top) or DPIX (bottom) 9 mmol L^{-1} Nd in dodecane+ 5 %$_{Vol}$ 1-octanol.
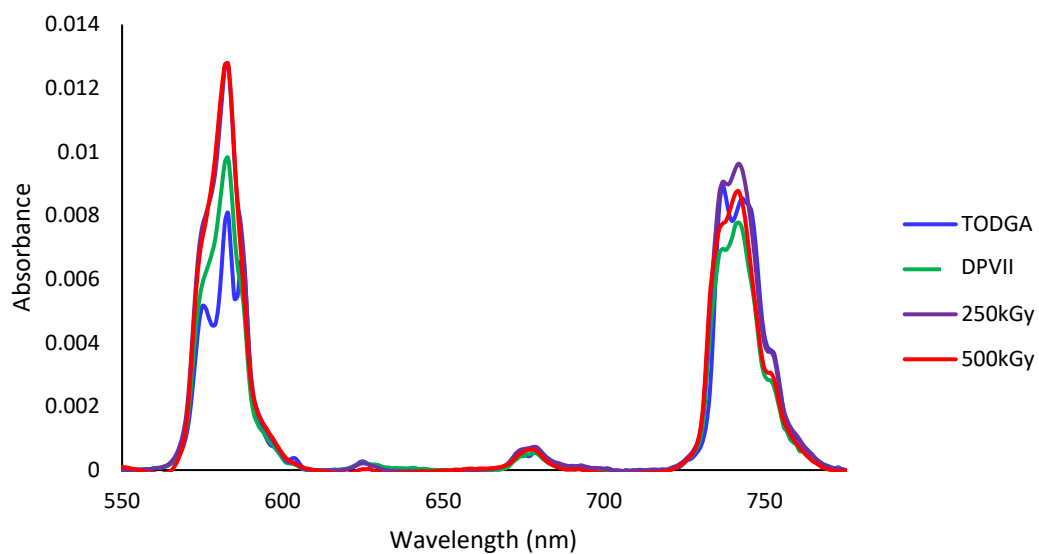
Figure S5. UV-Vis spectra comparing the Nd^{3+} spectra of irradiated TODGA solutions to the final titration of DPVII into a 0.1 mol L^{-1} TODGA in dodecane + 5 %$_{Vol}$ 1-octanol solution containing 15 mmol L^{-1} Nd. Ratio of TODGA to DPVII is 1:1. Spectra have been concentration / dilution corrected.
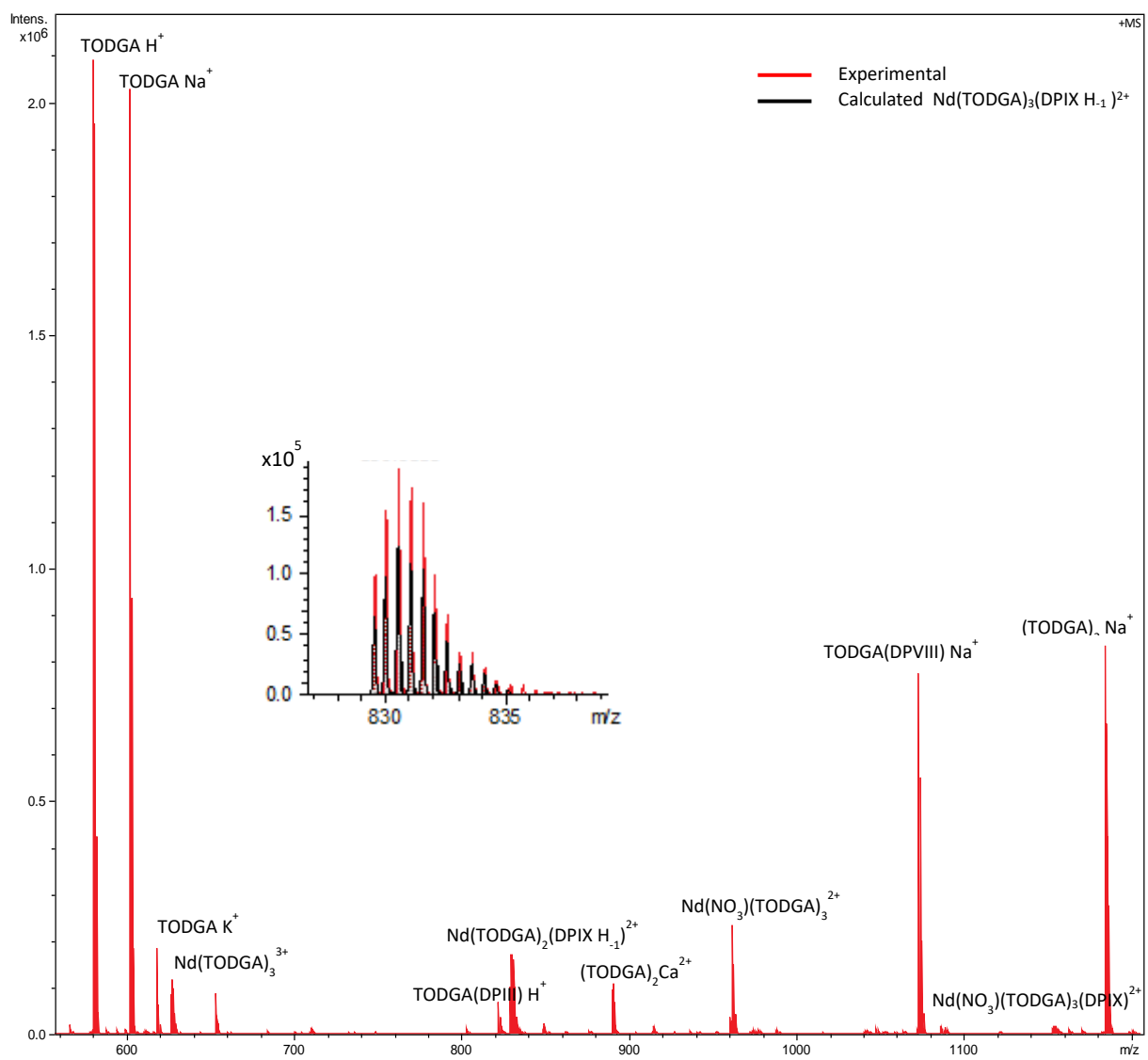
Figure S6: ESI-MS of the final titration solution of DPIX into Nd-TODGA in n-dodecane. The insert the largest peak containing DPIX and Nd. This peak only fits when DPIX is deprotonated.

References

1.	Y. Sugo, Y. Sasaki and S. Tachimori, *Radiochimica Acta*, 2002, **90**, 161-165.
2.	H. Galan, C. A. Zarzana, A. Wilden, A. Nunez, H. Schmidt, R. J. M. Egberink, A. Leoncini, J. Cobos, W. Verboom, G. Modolo, G. S. Groenewold and B. J. Mincher, *Dalton Transactions*, 2015, **44**, 18049-18056.
3.	H. Galan, A. Nunez, A. G. Espartero, R. Sedano, A. Durana and J. de Mendoza, *Procedia Chemistry*, 2012, **7**, 195-201.
4.	V. Hubscher-Bruder, V. Mogilireddy, S. Michel, A. Leoncini, J. Huskens, W. Verboom, H. Galan, A. Nunez, J. Cobos, G. Modolo, A. Wilden, H. Schmidt, M. C. Charbonnel, P. Guilbaud and N. Boubals, *New Journal of Chemistry*, 2017, **41**, 13700-13711.
5.	K. M. Roscioli-Johnson, C. A. Zarzana, G. S. Groenewold, B. J. Mincher, A. Wilden, H. Schmidt, G. Modolo and B. Santiago-Schübel, *Solvent Extraction and Ion Exchange*, 2016, **34**, 439-453.
6.	I. Sánchez-García, H. Galán, J. M. Perlado and J. Cobos, *EPJ Nuclear Sci. Technol.*, 2019, **5**, 19.
7.	J. N. Sharma, R. Ruhela, K. K. Singh, M. Kumar, C. Janardhanan, P. V. Achutan, S. Manohar, P. K. Wattal and A. K. Suri, *Radiochimica Acta*, 2010, **98**, 485-491.
8.	C. A. Zarzana, G. S. Groenewold, B. J. Mincher, S. P. Mezyk, A. Wilden, H. Schmidt, G. Modolo, J. F. Wishart and A. R. Cook, *Solvent Extraction and Ion Exchange*, 2015, **33**, 431-447.